Enhanced Skin Cancer Classification using Deep Learning and Nature-based Feature Optimization

Talha Imran

Department of Computer Science, COMSATS University Islamabad, Pakistan
itsmetalhaimran@gmail.com (corresponding author)

Ahmed S. Alghamdi

Department of Cybersecurity, College of Computer Science and Engineering, University of Jeddah, Saudi Arabia
ahmedg@uj.edu.sa

Mohammed Saeed Alkatheiri

Department of Cybersecurity, College of Computer Science and Engineering, University of Jeddah, Saudi Arabia
msalkatheri@uj.edu.sa

ABSTRACT

This paper presents a skin cancer classification model that combines a pre-trained Convolutional Neural Network (CNN) with a nature-inspired feature optimization algorithm. A custom dataset comprising both malignant and benign skin cancer microscopic illustrations is derived from the ISIC dataset of dermoscopic images. Several preprocessing steps are performed on the input pictures, such as histogram equalization, gamma correction, and white balance adjustment, to improve visibility, quality, and make color corrections. Deep feature extraction and pattern recognition are conducted on both enhanced and original dataset images using the pre-trained CNN model EfficientNetB0. As a result of fusing these features, the model can capture rich details from both dataset versions at the same time. Ant Colony Optimization (ACO), a nature-inspired feature selection algorithm is applied to perform model optimization by keeping the most relevant features and discarding the unnecessary ones. The optimized feature vector is then used with various SVM classifier kernels for the skin cancer classification task. The maximum achieved accuracy of the proposed model exceeded 98% through CB-SVM while maintaining an excellent prediction speed and reduced training time.

Keywords-skin cancer; deep learning; CNN; Ant Colony Optimization (ACO); classification

I. INTRODUCTION

Skin cancer occurs in the upper skin layer, which contains squamous cells, basal cells, and melanocytes. Skin cancers that do not involve the melanocytes, like squamous cell and basal cell types, can often be successfully treated and not spread. However, malignant melanoma, another cancer type, is more dangerous if not detected early [1]. Early melanoma detection can help cure them, but it can be very difficult to treat them if they spread further into the skin and other body parts. Melanoma development occurs when melanocytes, the pigment-producing cells in the skin, undergo harmful changes. In addition to containing brown or black shades, it can also exhibit pink, red, or purple colors when there is no pigment present. Skin cancer diagnosis can be improved through a variety of methods and computer systems such as the seven-point checklist and the ABCD rule [2]. Early melanoma detection is crucial, but it remains challenging even for specialists [3]. Detecting skin cancer early is essential for a high chance of recovery, but it can be costly due to the resemblance of skin lesions. Dermatologists often use expensive dermatoscopes for close examination. The effectiveness of dermoscopy is determined by the skill of the doctor, who uses special light and oil to examine beneath the skin. By analyzing color, shape, and texture, computers can assist doctors in diagnosing melanoma with greater accuracy. Recent advancements in computer vision allow for distinguishing between skin conditions without specialized devices, using common cameras to capture images, potentially improving early detection [4]. Detecting skin cancer at an early

stage, including melanoma, is vital to improving survival rates, especially in individuals with lighter skin tones. As a result, there is a growing demand for highly accurate automatic skin cancer detection systems. Two types of images are typically captured by these systems: dermatoscopy images captured by specialty equipment in pathology centers, which require dermatologist assessment, and digital images that can be taken at home using standard digital cameras. Nevertheless, it would be possible for individuals to perform skin cancer screenings conveniently and affordably in their own homes by utilizing software that automatically detects skin cancer from digital illustrations, without focusing too much on the Region of Interest (ROI) [5].

Numerous research papers have explored the use of image-processing techniques for the detection of melanoma skin cancer. This approach has several advantages, including the ability to quantify patient changes over time, generate image sets for educational purposes, facilitate rapid image comparison, and potentially offer cost savings [6]. Early diagnosis is paramount for successful skin cancer treatment, commonly achieved through the biopsy method. This process, while effective, presents drawbacks such as pain, time consumption, and delayed results. A viable alternative lies in computer-based technology, offering a more comfortable, cost-effective, and faster means of identifying potential skin cancer issues. Researchers advocate for non-invasive techniques involving digital image capture, preprocessing for analysis readiness, segmentation to isolate the region of interest, and feature extraction, considering factors like color, texture, and shape for distinguishing between benign and malignant lesions. According to the extracted features, the system uses Machine Learning (ML) algorithms like Support Vector Machines (SVMs) or Neural Networks (NNs) to classify the skin lesion as benign or malignant [7]. Deep Learning (DL) has profoundly transformed the ML landscape. It has demonstrated remarkable success in diverse fields, including speech recognition [8], pattern recognition [9], bioinformatics [10]. Moreover, it is increasingly applied to computer-based skin cancer detection, showcasing its potential to enhance accuracy and efficiency in this critical medical domain. Authors in [11] used ML and image processing to detect and classify different types of skin cancer. By implementing preprocessing, color-based segmentation, and feature extraction techniques, they achieved an impressive 96.25% accuracy on the ISIC 2019 Challenge dataset, demonstrating the effectiveness of these methods for early skin cancer detection. Authors in [12] conducted experiments with 640 skin lesion images from the ISIC archive, using 512 for training and the remaining for testing. While the Convolutional Neural Network (CNN) performed best, classical ML and image processing methods had their strengths, occasionally detecting melanoma when the CNN could not. To boost performance, they employed majority voting to combine results, improving melanoma detection. This paper introduces an optimized technique for skin cancer diagnosis using CNNs with enhanced Whale Optimization Algorithm (WOA) for weight and bias selection, reducing the network error. The method was tested on Dermquest and DermIS datasets, outperforming 10 other methods in terms of specificity, accuracy, sensitivity, NPV, and PPV. Current

Computer-Aided Diagnosis (CAD) systems face challenges in identifying melanoma due to the complex appearance of nevi.

Authors in [13] introduce an intelligent ROI system utilizing transfer learning, leveraging an improved k-means algorithm for ROI extraction. By focusing on discriminative features and using CNNs with data augmentation, the proposed approach achieved 97.9% and 97.4% accuracy on DermIS and DermQuest datasets, outperforming methods using complete images for classification. Authors in [14] aimed to create a CNN model for skin cancer diagnosis engaging lesion images. Data augmentation was employed as a preprocessing step to enhance model classification robustness. The top-performing model, InceptionResnet, achieved an average accuracy of 91%. Authors in [15] addressed challenges in dermoscopy image lesion detection by proposing a lightweight skin cancer recognition model based on fine-grained classification principles. The model incorporates feature extraction and discrimination modules, leveraging positive and negative sample pairs. It efficiently extracts discriminative lesion features, upgrading recognition performance with minimal parameters. Additionally, it enables precise lesion area segmentation utilizing a U-Net architecture and migration training strategy, outperforming existing DL-based methods on the ISBI 2016 skin lesion analysis dataset. Authors in [16] addressed the challenge of automating the localization and segmentation of early-stage melanoma skin cancer lesions. They proposed a method that employed Faster Region-based Convolutional Neural Networks (RCNNs) and Fuzzy K-Means (FKM) clustering for segmentation. The approach preprocesses images to enhance visual information, applies Faster-RCNN for feature extraction, and employs FKM for variable-sized lesion segmentation. The method achieved high accuracy of 95.40%, 93.1%, and 95.6% on ISIC-2016, ISIC-2017, and PH2 datasets, respectively, outperforming state-of-the-art approaches and making it a robust tool for skin lesion recognition and segmentation. Authors in [17] used the ISIC2018 dataset with 3533 skin lesions, ameliorating images with ESRGAN and applying CNNs for classification. Multiple transfer learning models, including Resnet50, InceptionV3, and Inception Resnet, were fine-tuned and utilized. The CNN achieved 83.2% accuracy, comparable to other models, highlighting this approach effectiveness at skin lesion detection.

Skin cancer recognition from medical images remains an active research area, with recent focus on DL neural networks. Authors in [18] present 11 CNN architectures trained and tested on the HAM10000 dataset for 7 skin lesion classes. Data augmentation, transfer learning, and fine-tuning addressed imbalance and similarity issues, with DenseNet169 yielding the best results (92.25% accuracy, 93.59% recall, 93.27% F1-score), surpassing state-of-the-art methods. A lightweight version of DenseNet169 was integrated into a mobile Android app for real-time classification of skin lesions and personalized sun exposure recommendations based on UV radiation and skin type. Authors in [19] focused on lung cancer classification using a dataset of 3600 images (224 × 224 pixels) divided into two classes: malignant and benign. A CNN with fully connected layers was employed, resulting in an accuracy of 86.23% with efficient computations.

This paper proposes a hybrid model for skin cancer classification, comprising image processing techniques, a pre-trained CNN, and a nature-based feature optimization algorithm. The main stages of the current work are:

- Histogram equalization, gamma correction, and white balance adjustment, which are among the preprocessing techniques adopted to enhance the original dataset images.

- Features are extracted by the pre-trained EfficientNetB0 for both the original dataset and its post-enhancement version, which were then serially fused on making the model more flexible in terms of learning and adaptation.

- The extracted features from both scenarios were withdrawn from the last fully connected layer of the EfficientNetB0, and were optimized using ACO.

- The optimized feature vector was then provided as an input to various SVM classifier kernels, and classification was carried out.

II. REGARDING THE CONTENT

This paper proposes a model for skin cancer classification based on the hybrid application of a pre-trained CNN and a nature-based feature optimization algorithm. The proposed model architecture is shown in Figure 1.
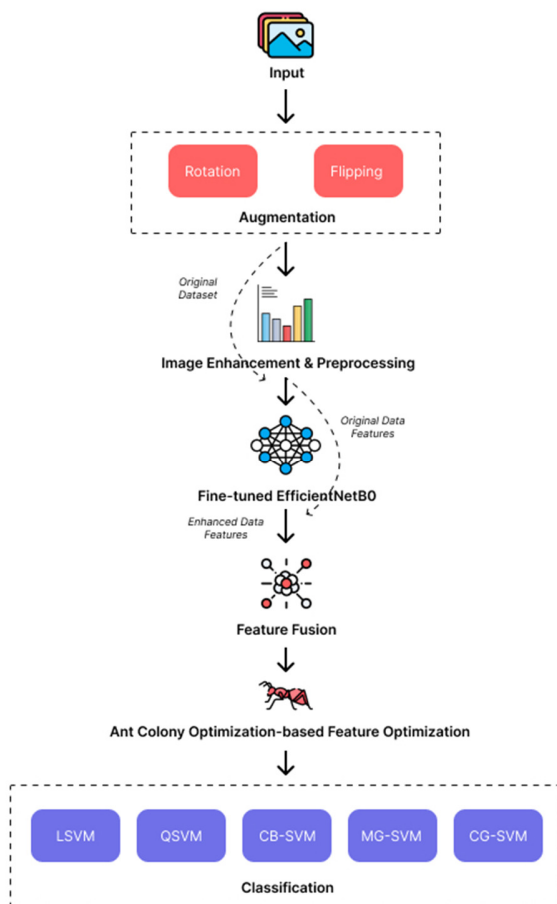

Fig. 1. Overview of proposed model.

A custom dataset is developed comprising of microscopic images of malignant and benign skin cancer classes, extracted from the ISIC dataset of dermoscopic images. Preprocessing techniques including histogram equalization, gamma correction, and white balance adjustment are applied on the input images with regard to each of their individual R, G, and B channels to make them more prominent, perform color correction, and enhance their overall geometry. The pre-trained CNN EfficientNetB0 is used for pattern recognition and deep feature extraction from the enhanced dataset images. The features elicited by the EfficientNetB0 are then serially fused with the features educed by it when operating on pre-enhancement dataset. This is done to enable the model to absorb details from both the original images and their enhanced versions. To reduce the overall dimension complexity of the fused features, ACO, a nature-based feature selection algorithm, is applied on the latter. ACO eliminates the complexity of the fused feature vector by selecting the most relevant features and discarding the less significant ones. The optimized feature vector is then provided to various SVM classifier kernels to perform classification. The proposed model achieved a maximum accuracy of over 98% while maintaining an excellent prediction speed and reduced training time.

A. Dataset

The dataset used in this work is International Skin Imaging Collaboration (ISIC), which is a global organization dedicated to advancing skin cancer diagnosis and management [20]. The creators have gathered a large collection of skin images, including moles and lesions, for training AI systems to improve diagnosis precision. The primary goal of ISIC is to provide healthcare professionals with cutting-edge tools for early skin cancer identification, which is essential for successful treatment. The ISIC 2019 dataset [21] includes over 25,000 skin lesion images covering various categories, including skin cancer types, benign lesions, and other dermatological conditions. ISIC 2020 also had a significant number of images, but the number of classes and images varied depending on specific challenges. ISIC datasets evolve with new versions and challenges to advance dermatology and skin cancer diagnosis research and development. For this work, a custom dataset is developed comprising microscopic images of malignant and benign skin cancer classes, extracted from the ISIC dataset.

B. Preprocessing

Histogram equalization was first applied at this stage [22]. It improves contrast and brightness by rearranging pixel values within an image to generate a more uniform distribution. This technique is useful for upgrading image quality, particularly in low-contrast or poorly lit situations. To address image quality degradation due to device limitations or unfavorable conditions, we categorized the images based on statistical characteristics and applied Adaptive Gamma Correction (AGC) [23] to dynamically adjust parameters, significantly enhancing contrast. To further ameliorate image quality, we employed a technique known as automatic white balancing [24], which plays a crucial role in digital photography by significantly improving image quality. A novel algorithm, which adjusts adjacent color channels, using luminance and RGB component standard deviation, and includes a light source model for

evaluation, is introduced. Simulations confirm its effectiveness in improving the final image quality. Figure 2 depicts a comparison of the dataset before and after the preprocessing step.
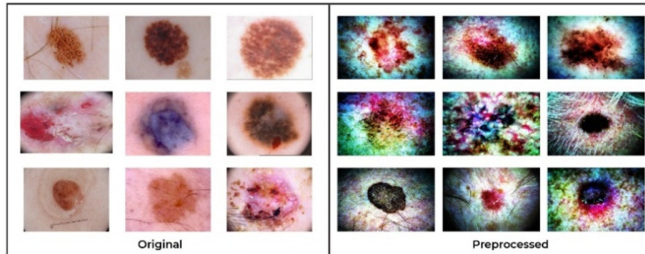

Fig. 2.   Comparison of dataset scenarios: (a) Original, (b) preprocessed.

C. Feature Extraction using EfficientNetB0

In the feature extraction step, both the original and the preprocessed datasets pass through the pre-trained EfficientNetB0, and features are extracted from both as shown in Table I. EfficientNetB0 has already learned useful information from datasets like ImageNet, and hence can absorb further details from the given dataset. In this case, it is initialized with pre-trained weights and bias, the extracted features are taken out of the last fully connected layer for optimization and classification. The classifiers are trained by providing the features as input, and give benign/malignant labels as output. The system performance is evaluated by metrics such as accuracy, precision, recall, and f1-score. Optionally, the model can be further fine-tuned to provide predictions on the specific skin cancer dataset and its performance can be enhanced, but the proposed work did not focus on CNN fine tuning. Pre-trained CNNs are vastly used to aid early skin cancer detection, ensure ethical and regulatory compliance, and validate the system on diverse datasets to ensure reliability and generalizability [25].

TABLE I.   PRE AND POST FEATURE SELECTION OVERVIEW

Original dataset features	Preprocessed dataset features
20,000 × 1,000	20,000 × 1,000

D. Feature Fusion

A key step in image processing is feature fusion, which merges data from several sources to enhance feature representation and discriminative ability for more thorough image analysis. The two basic approaches of feature fusion techniques are the serial and parallel methods. The serial approach integrates features sequentially, while the parallel method does so simultaneously, making use of parallel processing for faster fusion. We extracted deep features from the last fully connected layer of the CNN for both datasets and merged them using the serial-based fusion method. This fused feature vector retains information from the same dataset under two different conditions. We optimized this vector by removing redundant and useless information while preserving important details. This optimization involves data augmentation and three preprocessing techniques on the enhanced dataset, followed by

feature extraction using CNN. At the same time, we provided the dataset before preprocessing to EfficientNetB0. Finally, we serially fused the derived feature vectors from both cases to create a compact 20,000×2,000 feature vector.

E. Feature Selection and Optimization

Swarm intelligence allows us to observe the social behaviors of animals and insects, inspiring creative problem-solving ideas for our daily lives. ACO [26] is a prime example, offering insights into how ants forage for food. Ants communicate by leaving pheromone trails on the ground, guiding other colony members to follow these paths. This unique communication method, known as stigmergy, is essential for the blind ants to coordinate effectively. Pheromones, chemical substances produced by animals, play a crucial role in shaping the behavior of their fellow species members. Equation (1) shows the pheromone level in a graph.

$$\Delta\tau_{i,j}^{k} = \begin{cases} \frac{1}{L_k} \\ 0 \end{cases} \tag{1}$$

where τ represents the amount of pheromone deposited by an ant on an edge connecting two nodes, i and j, in a graph. The variable k signifies the kth ant in the colony. The term $\Delta\tau_{i,j}^{k}$ represents the change in pheromone levels deposited by the Kth ant on that specific edge. The division by L_k is crucial because it reflects the length of the path found by the kth ant. A shorter path found by an ant leads to a higher amount of pheromone being deposited on that path. Essentially, this equation encourages ants to favor shorter paths by depositing more pheromone on them, ultimately helping the colony converge towards finding the shortest and most efficient route.

Equation (1) describes the behavior of a single ant, but we have adopted it for multiple ants in this scenario. Instead of considering a single ant, we now use a summation to calculate the cumulative pheromone level on each edge. Unlike situations where pheromone evaporates, here, pheromone accumulates over time as multiple ants contribute to it. The primary objective remains unchanged: shorter paths receive more pheromone, guiding the colony toward efficient solutions.

$$\tau_{i,j}^{k} = \sum_{k=1}^{m} \Delta\tau_{i,j}^{k} \tag{2}$$

In (2), m denotes the total number of ants. $\tau_{i,j}^{k}$ represents the current pheromone status and the new pheromone that should be deposited by all ends. Here, vaporization occurs because experiments cycle is performed once by all ants on all the graph edges.

$$\tau_{i,j}^{k} = (1-\rho)\,\tau_{i,j}^{k} + \sum_{k=1}^{m} \Delta\tau_{i,j}^{k} \tag{3}$$

In (3), (1-ρ) denotes the current pheromone level, whereas ρ represents the constant value, and defines the evaporation rate. EfficientNetB0 has been employed for feature extraction. The extraction process can result in redundant features that impact both time and accuracy. To address this issue, we have integrated the ACO selection algorithm. ACO helps select only the most relevant features, enhancing both efficiency and accuracy of the proposed model. ACO operates during the feature selection process, leveraging its mechanisms to optimize feature selection and improve the overall performance

of the proposed skin cancer detection system. Table II shows the process of feature selection using ACO.

TABLE II.   FEATURE OVERVIEW, PRE AND POST FEATURE SELECTION

Features Pre-ACO	Features Post-ACO
20,000 × 2,000	20,000 × 200

F. Classification

The main aim of the proposed work is to perform skin cancer classification. Predefined labels to images based on their visual content are assigned. To conduct the classification, several SVM classifier kernels are employed namely Linear SVM (LSVM), Quadratic SVM (QSVM), Cubic SVM (CB-SVM), Medium Gaussian SVM (MG-SVM), and Coarse Gaussian SVM (CG-SVM). After extracting the right features from the images in the previous feature optimization step, these features with labels are used to train the SVM classifiers. The SVM kernels learn from these labeled features, picking up on patterns and traits that help identify specific classes. Once they are trained, the SVM classifiers make predictions, and we assess their performance in the next section. This evaluation is based on certain performance measures to see how well each kernel can classify images.

III.   THE PROPOSED CLASSIFICATION METHODOLOGY

This paper presents a skin cancer classification model from dermoscopic images that combines EfficientNetB0, a pre-trained CNN, with ACO algorithm. It uses a custom dataset derived from the ISIC dataset, and applies preprocessing techniques for improved image quality. The model extracts features from both the original and enhanced dataset versions, reducing dimension complexity with ACO before classifying the optimized features, using various SVM kernels. A total of four experiments were performed to validate the model based on various dataset and methodology combinations. All the experiments are discussed in detail in the following sections. The system used for all the experimentation runs consisted of an Intel Core i5-4210U CPU with clock speed of 1.70 GHz, 12 GB DDR3 RAM, and 256 GB SSD. All the experiments were performed on MATLAB R2023a.

A. Experiment 1

In the first experiment, the original dataset consisting of 20,000 images was equally divided into two classes based on skin cancer severity, namely Malignant and Benign. These were provided as input to the pre-trained EfficientNetB0. Just like other CNNs, EfficientNetB0 employs its deep layers to extract features from the input images by applying a series of convolutional and pooling operations. These layers learn to detect and represent hierarchical visual patterns from simple edges and textures in early layers to complex infected regions and high-level features in deeper layers. The features are then extracted from the last fully connected layer of EfficientNetB0, named MatMul, organized in the form of a compact 20,000 × 1,000 feature vector, and passed on to SVM classifier and its various kernels for classification. Table III shows the result evaluation of the 5 SVM kernels.

TABLE III.   RESULT EVALUATION OF THE SVM CLASSIFIERS

Classifier	Accuracy (%)	Precision (%)	Recall (%)	F1-score (%)	Sensitivity (%)	Specificity (%)	MCC (%)
L-SVM	82.73	83.50	82.22	82.86	82.23	83.24	65.46
Q-SVM	93.52	94.43	92.74	93.58	92.74	94.33	87.05
CB-SVM	97.40	98.01	96.82	97.42	96.83	97.99	94.81
MG-SVM	94.11	94.86	93.44	94.15	93.45	94.78	88.22
CG-SVM	80.03	81.23	79.32	80.27	79.33	80.77	60.08

It can be clearly seen that CB-SVM performs better than the other classifiers with an elevated accuracy of 97.40%. Figure 3 shows the confusion matrix of the CB-SVM.
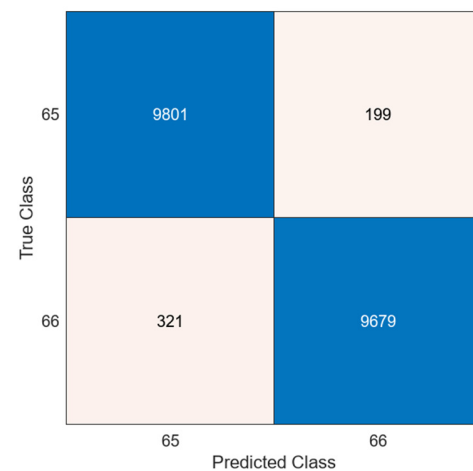

Fig. 3.   Confusion matrix of the CB-SVM in Experiment 1.

B. Experiment 2

In the second experiment, the original dataset consisting of 20,000 images, was equally divided into two classes based on skin cancer severity, namely Malignant and Benign passed through certain image enhancement and preprocessing steps including color balancing, gamma correction and white balance adjustment. This is done to enhance image quality, make the infected regions more prominent and correct the dullness issue in original dataset images. The improved dataset was then provided as an input to the pre-trained EfficientNetB0. These images were again fed to the EfficientNetB0 and its output to the SVM classifiers. Table IV shows the result evaluation of 5 SVM kernels.

TABLE IV.   RESULT EVALUATION OF SVM CLASSIFIERS

Classifier	Accuracy (%)	Precision (%)	Recall (%)	F1-score (%)	Sensitivity (%)	Specificity (%)	MCC (%)
L-SVM	78.06	79.71	77.16	78.42	77.16	79.02	56.15
Q-SVM	92.05	93.54	90.82	92.16	90.82	93.34	84.13
CB-SVM	96.77	97.78	95.84	96.80	95.84	97.73	93.56
MG-SVM	92.85	94..42	91.53	92.96	91.54	94.24	85.73
CG-SVM	75.13	77.86	73.82	75.79	73.82	76.58	50.33

CB-SVM again performs better than the rest classifiers with an accuracy of 96.77%. Figure 4 demonstrates the confusion matrix of CB-SVM. It can be noticed that even after preprocessing, the model fails to achieve higher accuracy. Its performance significantly decreases, instead, as compared to Experiment 1 where original dataset is used for experimentation. Therefore, it shows that preprocessing does not have any significant effect on the formulated model.
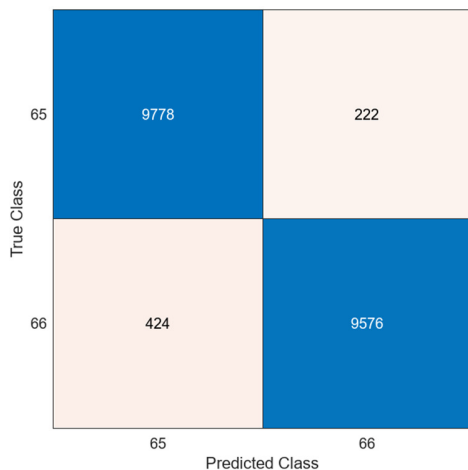

Fig. 4.   Confusion matrix of CB-SVM in Experiment 2.

C. Experiment 3

As it is evident from Experiment 1 and Experiment 2, the model is not able to achieve accuracy higher than 97.40%. Even after preprocessing, the performance slightly decrements rather than getting incremented. Therefore, the third experiment implements the feature fusion technique that enables the proposed model to capture complementary information and consider a broader range of image characteristics. This integration of diverse features leads to improved discrimination and generalization, making the model more robust and effective in skin cancer classification and recognition. In this experiment, the features extracted by the EfficientNetB0 from the original dataset in case of Experiment 1 are serially fused with the features extracted by the CNN from the preprocessed dataset of Experiment 2. This fusion leads to the generation of a new feature vector with dimensions of 20000×2000 that has obtained vast information from the same dataset in both original and enhanced condition. This feature vector is then provided to multiple SVM classifier kernels, and classification is performed. Table V shows the result evaluation of 5 SVM kernels.

TABLE V.   RESULT EVALUATION OF SVM CLASSIFIERS

Classifier	Accuracy (%)	Precision (%)	Recall (%)	F1-score (%)	Sensitivity (%)	Specificity (%)	MCC (%)
L-SVM	85.78	86.14	85.51	85.83	85.52	86.04	71.55
Q-SVM	98.34	99.76	96.99	98.36	97.00	99.75	96.71
CB-SVM	99.01	99.95	98.09	99.01	98.10	99.95	98.03
MG-SVM	98.62	99.87	97.43	98.64	97.43	99.87	97.27
CG-SVM	86.91	87.54	86.44	86.99	86.44	87.38	73.82

It can be seen that after conducting feature fusion, the overall performance of all the classifiers has improved to a great extent and the model has gained a noticeable increment in its performance. All models perform better in case of Experiment 3, but CB-SVM still performs better than the other classifiers with an accuracy exceeding 99%. Figure 5 depicts the confusion matrix of CB-SVM 3.
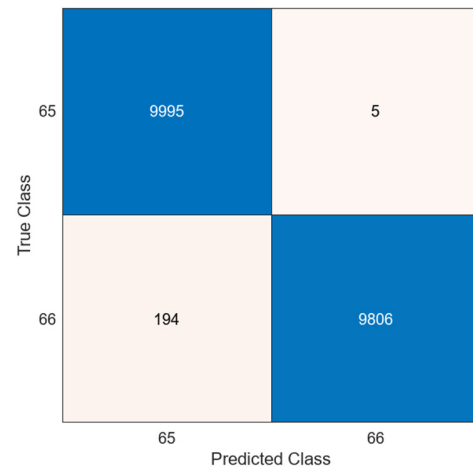

Fig. 5.   Confusion matrix of CB-SVM in Experiment 3.

This experiment proves that the proposed model performs better bon skin cancer classification when feature fusion is merged with the preprocessing techniques and CNN. Table VI presents the prediction speed and training time taken by all the SVM kernels in case of Experiment 3.

TABLE VI.   PREDICTION SPEED AND TRAINING TIME OF SVM CLASSIFIERS

Classifier	Prediction speed (obs/s)	Training time (s)
L-SVM	110	2086.3
Q-SVM	240	858.14
CB-SVM	280	704.58
MG-SVM	160	1206.8
CG-SVM	80	2558.6

D. Experiment 4

After achieving the efficient performance objective, the next goal is to make the model optimized so that it delivers accurate results while maintaining high speed and minimum time consumption. Therefore, the final experiment uses ACO to optimize the fused feature vector formulated in Experiment 3. ACO utilizes a population of artificial ants to explore and evaluate different feature combinations. Ants deposit pheromones to communicate with each other, guiding the search towards more promising feature subsets. Over time, ACO converges towards an optimal or near-optimal feature vector by favoring paths with higher pheromone concentrations, effectively selecting the most relevant features for a given task. In Experiment 4, the ACO is initialized with a population of 10, and the number of iterations is set to 15. The fused 20,000×2,000 feature vector is passed on as a problem space vector to the algorithm. ACO optimizes the feature

vector to 20,000×200 by selecting only the 200 most relevant features, and discards the rest. Table VII shows the result evaluation of 5 SVM kernels in Experiment 4. Just like the previous experiments, CB-SVM also turns out to be the best performing model in Experiment 4 with an accuracy of 98.43%. Figure 6 shows its confusion matrix f.

TABLE VII.   RESULT EVALUATION OF SVM CLASSIFIERS

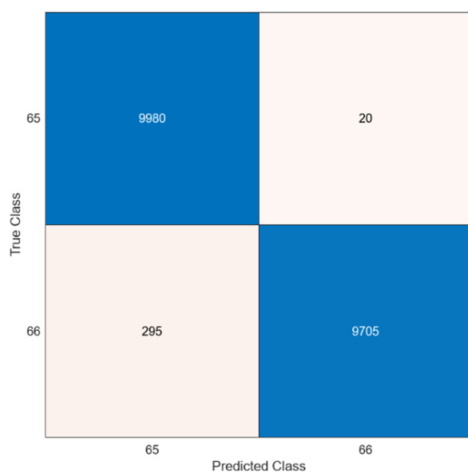| Classifier	Accuracy (%)	Precision (%)	Recall (%)	F1-Score (%)	Sensitivity (%)	Specificity (%)	MCC (%)
L-SVM	76.91	77.75	76.46	77.10	76.47	77.37	53.83
Q-SVM	97.37	99.41	95.51	97.42	95.51	99.38	94.82
CB-SVM	98.43	99.80	97.12	98.45	97.13	99.79	96.89
MG-SVM	97.98	99.69	96.38	98.01	96.38	99.68	96.01
CG-SVM	82.50	83.71	81.73	82.71	81.73	93.31	65.02

Fig. 6.   Confusion matrix of CB-SVM in Experiment 4.

Table VIII illustrates the prediction speed and training time taken by all the SVM kernels in Experiment 4. It can be observed that the time consumed by the classifiers while providing prediction on fused features and the prediction speed were quite improved.

TABLE VIII.   RESULTS EVALUATION OF SVM CLASSIFIERS BASED ON PERFORMANCE MEASURES

Classifier	Prediction speed (obs/s)	Training time (s)
L-SVM	860	317.94
Q-SVM	2500	153.66
CB-SVM	2600	125.06
MG-SVM	1500	180.63
CG-SVM	600	388.53

IV.   DISCUSSION

The proposed model performed best in case of Experiment 3 with accuracy of CB-SCM exceeding 99%. But this increase in accuracy brought along some downsides in terms of reduced prediction speed and higher training time. Having a classifier with slower prediction speed and longer training time can be disadvantageous in real-time applications because it may lead to delayed responses. It can also increase computational resource requirements, making it less suitable for resource-

constrained environments. Data optimization is crucial as it reduces the dimensionality and noise in the dataset, making the training process more efficient. It also improves the classifier performance by focusing on the most relevant information. This leads to faster training times and quicker predictions, making the classifier more practical for real-time use or large-scale applications. Therefore, ACO feature optimization algorithm is embedded into the proposed model. Its effectiveness can be seen in Experiment 4, which shows that CB-SVM achieved 98.43% accuracy. It may be less impressive than the accuracy of 99.01% in Experiment 3, but is still very high. Therefore, by achieving almost the same performance, ACO helped the model to greatly increase prediction speed as illustrated in Figure 7.
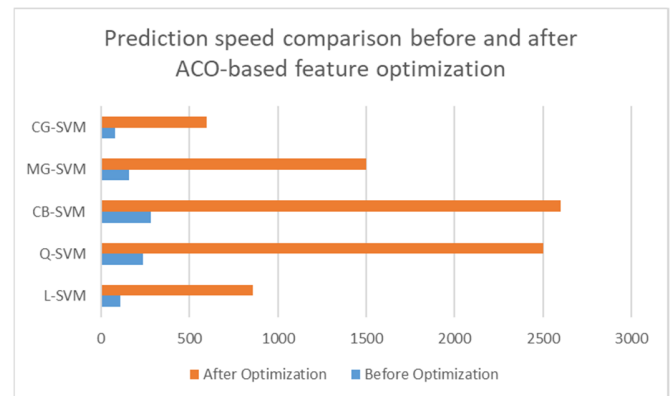

Fig. 7.   Prediction speed before and after ACO-based feature optimization.

After the implementation of ACO, the model's overall training time also got reduced to a great extent. The time consumed by the classifier kernels on optimized features is far less than that on non-optimized features as shown in Figure 8.
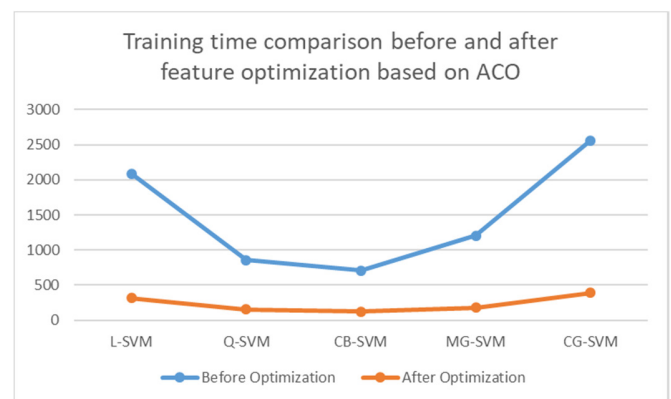

Fig. 8.   Training time before and after ACO-based feature optimization.

The proposed model indicates that feature fusion when integrated with certain image enhancement techniques and a fine-tuned CNN model, can lead to better accuracy but with compromise on time and speed. Appropriate feature selection algorithms can help solve the issue related to training time and prediction speed and an overall accurate yet slick model can be developed. The future research can focus on leveraging custom

CNN models for skin cancer classification, and exploring better feature selection algorithms to achieve this. Table IX illustrates a comparison of some of the latest existing works with the proposed work. It can be seen that the proposed model excels in terms of accuracy.

TABLE IX.   ACCURACY COMPARISON WITH EXISTING WORKS

Reference	Year	Accuracy (%)
[28]	2020	92.83
[31]	2020	95.34
[29]	2021	91.93
[30]	2021	93.7
[27]	2022	87.91
[32]	2023	89.57
Proposed	2023	98.43

V.   CONCLUSION

The current paper presents an innovative approach to skin cancer classification, leveraging the synergistic combination of a pre-trained CNN (EfficientNetB0) and a nature-based feature optimization algorithm (ACO). Through the development of a custom dataset and meticulous preprocessing techniques, the model excels in extracting meaningful features from microscopic malignant and benign skin cancer images. Feature fusion from both the original and enhanced images significantly enhances model capacity for pattern recognition. By applying ACO for dimensionality reduction, the model optimizes feature selection, ultimately resulting in a highly accurate classification system, achieving an accuracy rate exceeding 98%. Finally, this accuracy is attained without compromising prediction speed and training time, making it a promising tool for real-world applications in dermatology and medical image analysis.

ACKNOWLEDGMENT

REFERENCES

[1]   U. B. Ansari and T. Sarode, "Skin Cancer Detection Using Image Processing," *International Research Journal of Engineering and Technology*, vol. 4, no. 4, pp. 2875–2881, 2017.

[2]   S. Jain, V. jagtap, and N. Pise, "Computer Aided Melanoma Skin Cancer Detection Using Image Processing," *Procedia Computer Science*, vol. 48, pp. 735–740, Jan. 2015, https://doi.org/10.1016/j.procs.2015.04.209.

[3]   N. Zhang, Y.-X. Cai, Y.-Y. Wang, Y.-T. Tian, X.-L. Wang, and B. Badami, "Skin cancer diagnosis based on optimized convolutional neural network," *Artificial Intelligence in Medicine*, vol. 102, Jan. 2020, Art. no. 101756, https://doi.org/10.1016/j.artmed.2019.101756.

[4]   P. Dubal, S. Bhatt, C. Joglekar, and S. Patil, "Skin cancer detection and classification," in *6th International Conference on Electrical Engineering and Informatics*, Langkawi, Malaysia, Nov. 2017, pp. 1–6, https://doi.org/10.1109/ICEEI.2017.8312419.

[5]   E. Jana, R. Subban, and S. Saraswathi, "Research on Skin Cancer Cell Detection Using Image Processing," in *International Conference on Computational Intelligence and Computing Research*, Coimbatore, India, Dec. 2017, pp. 1–8, https://doi.org/10.1109/ICCIC.2017.8524554.

[6]   H. Alquran *et al.*, "The melanoma skin cancer detection and classification using support vector machine," in *Jordan Conference on Applied Electrical Engineering and Computing Technologies*, Aqaba, Jordan, Oct. 2017, pp. 1–5, https://doi.org/10.1109/AEECT.2017.8257738.

[7]   M. Dildar *et al.*, "Skin Cancer Detection: A Review Using Deep Learning Techniques," *International Journal of Environmental Research and Public Health*, vol. 18, no. 10, Jan. 2021, Art. no. 5479, https://doi.org/10.3390/ijerph18105479.

[8]   U. Kamath, J. Liu, and J. Whitaker, *Deep learning for NLP and speech recognition*. New York, NY, USA: Springer, 2019.

[9]   J. Ker, L. Wang, J. Rao, and T. Lim, "Deep Learning Applications in Medical Image Analysis," *IEEE Access*, vol. 6, pp. 9375–9389, 2018, https://doi.org/10.1109/ACCESS.2017.2788044.

[10]   Y. Cao, T. A. Geddes, J. Y. H. Yang, and P. Yang, "Ensemble deep learning in bioinformatics," *Nature Machine Intelligence*, vol. 2, no. 9, pp. 500–508, Sep. 2020, https://doi.org/10.1038/s42256-020-0217-y.

[11]   M. K. Monika, N. Arun Vignesh, Ch. Usha Kumari, M. N. V. S. S. Kumar, and E. L. Lydia, "Skin cancer detection and classification using machine learning," *Materials Today: Proceedings*, vol. 33, pp. 4266–4270, Jan. 2020, https://doi.org/10.1016/j.matpr.2020.07.366.

[12]   J. Daghrir, L. Tlig, M. Bouchouicha, and M. Sayadi, "Melanoma skin cancer detection using deep learning and classical machine learning techniques: A hybrid approach," in *5th International Conference on Advanced Technologies for Signal and Image Processing*, Sousse, Tunisia, Sep. 2020, pp. 1–5, https://doi.org/10.1109/ATSIP49331.2020.9231544.

[13]   R. Ashraf *et al.*, "Region-of-Interest Based Transfer Learning Assisted Framework for Skin Cancer Detection," *IEEE Access*, vol. 8, pp. 147858–147871, 2020, https://doi.org/10.1109/ACCESS.2020.3014701.

[14]   H. Nahata and S. P. Singh, "Deep Learning Solutions for Skin Cancer Detection and Diagnosis," in *Machine Learning with Health Care Perspective: Machine Learning and Healthcare*, V. Jain and J. M. Chatterjee, Eds. New York, NY, USA: Springer, 2020, pp. 159–182.

[15]   L. Wei, K. Ding, and H. Hu, "Automatic Skin Cancer Detection in Dermoscopy Images Based on Ensemble Lightweight Deep Learning Network," *IEEE Access*, vol. 8, pp. 99633–99647, 2020, https://doi.org/10.1109/ACCESS.2020.2997710.

[16]   M. Nawaz *et al.*, "Skin cancer detection from dermoscopic images using deep learning and fuzzy k-means clustering," *Microscopy Research and Technique*, vol. 85, no. 1, pp. 339–351, 2022, https://doi.org/10.1002/jemt.23908.

[17]   W. Gouda, N. U. Sama, G. Al-Waakid, M. Humayun, and N. Z. Jhanjhi, "Detection of Skin Cancer Based on Skin Lesion Images Using Deep Learning," *Healthcare*, vol. 10, no. 7, Jul. 2022, Art. no. 1183, https://doi.org/10.3390/healthcare10071183.

[18]   I. Kousis, I. Perikos, I. Hatzilygeroudis, and M. Virvou, "Deep Learning Methods for Accurate Skin Cancer Recognition and Mobile Application," *Electronics*, vol. 11, no. 9, Jan. 2022, Art. no. 1294, https://doi.org/10.3390/electronics11091294.

[19]   A. Atta, M. A. Khan, M. Asif, G. F. Issa, R. A. Said, and T. Faiz, "Classification of Skin Cancer empowered with convolutional neural network," in *International Conference on Cyber Resilience*, Dubai, United Arab Emirates, Oct. 2022, pp. 01–06, https://doi.org/10.1109/ICCR56254.2022.9995928.

[20]   N. Codella *et al.*, "Skin Lesion Analysis Toward Melanoma Detection 2018: A Challenge Hosted by the International Skin Imaging Collaboration (ISIC)." arXiv, Mar. 29, 2019, https://doi.org/10.48550/arXiv.1902.03368.

[21]   M. A. Kassem, K. M. Hosny, and M. M. Fouad, "Skin Lesions Classification Into Eight Classes for ISIC 2019 Using Deep Convolutional Neural Network and Transfer Learning," *IEEE Access*, vol. 8, pp. 114822–114832, 2020, https://doi.org/10.1109/ACCESS.2020.3003890.

[22]   S. S. Bagade and V. K. Shandilya, "Use of histogram equalization in image processing for image enhancement," *International Journal of Software Engineering Research & Practices*, vol. 1, no. 2, pp. 6–10, 2011.

[23]   S. Rahman, M. M. Rahman, M. Abdullah-Al-Wadud, G. D. Al-Quaderi, and M. Shoyaib, "An adaptive gamma correction for image

enhancement," *EURASIP Journal on Image and Video Processing*, vol. 2016, no. 1, Oct. 2016, Art. no. 35, https://doi.org/10.1186/s13640-016-0138-1.

[24] H.-K. Lam, O. C. Au, and C.-W. Wong, "Automatic white balancing using adjacent channels adjustment in RGB domain," in *International Conference on Multimedia and Expo (ICME) (IEEE Cat. No.04TH8763)*, Taipei, Taiwan, Jun. 2004, vol. 2, pp. 979-982 Vol.2, https://doi.org/10.1109/ICME.2004.1394366.

[25] M. Tan and Q. Le, "EfficientNet: Rethinking Model Scaling for Convolutional Neural Networks," in *36th International Conference on Machine Learning*, Long Beach, CA, USA, Jun. 2019, pp. 6105–6114.

[26] M. Dorigo, M. Birattari, and T. Stutzle, "Ant colony optimization," *IEEE Computational Intelligence Magazine*, vol. 1, no. 4, pp. 28–39, Aug. 2006, https://doi.org/10.1109/MCI.2006.329691.

[27] K. Ali, Z. A. Shaikh, A. A. Khan, and A. A. Laghari, "Multiclass skin cancer classification using EfficientNets – a first step towards preventing skin cancer," *Neuroscience Informatics*, vol. 2, no. 4, Dec. 2022, Art. no. 100034, https://doi.org/10.1016/j.neuri.2021.100034.

[28] S. S. Chaturvedi, J. V. Tembhurne, and T. Diwan, "A multi-class skin Cancer classification using deep convolutional neural networks," *Multimedia Tools and Applications*, vol. 79, no. 39, pp. 28477–28498, Oct. 2020, https://doi.org/10.1007/s11042-020-09388-2.

[29] M. S. Ali, M. S. Miah, J. Haque, M. M. Rahman, and M. K. Islam, "An enhanced technique of skin cancer classification using deep convolutional neural network with transfer learning models," *Machine Learning with Applications*, vol. 5, Sep. 2021, Art. no. 100036, https://doi.org/10.1016/j.mlwa.2021.100036.

[30] S. K. Datta, M. A. Shaikh, S. N. Srihari, and M. Gao, "Soft Attention Improves Skin Cancer Classification Performance," in *International Workshop on Interpretability of Machine Intelligence in Medical Image Computing*, Strasbourg, France, Sep. 2021, pp. 13–23, https://doi.org/10.1007/978-3-030-87444-5_2.

[31] S. S. Chaturvedi, K. Gupta, and P. S. Prasad, "Skin Lesion Analyser: An Efficient Seven-Way Multi-class Skin Cancer Classification Using MobileNet," in *International Conference on Advanced Machine Learning Technologies and Applications*, Cairo, Egypt, Mar. 2021, pp. 165–176, https://doi.org/10.1007/978-981-15-3383-9_15.

[32] S. Qasim Gilani, T. Syed, M. Umair, and O. Marques, "Skin Cancer Classification Using Deep Spiking Neural Network," *Journal of Digital Imaging*, vol. 36, no. 3, pp. 1137–1147, Jun. 2023, https://doi.org/10.1007/s10278-023-00776-2.